

Hypersonic Model Testing in a Shock Tunnel

H. Olivier* and H. Grönig†
RWTH Aachen, 52056 Aachen, Germany
and

A. Le Bozec‡
Dassault Aviation, 78141 Vélizy-Villacoublay, France

A shock tunnel is used to perform tests at hypersonic flow conditions including weak real gas effects. Pressure and heat flux distributions are measured around typical re-entry configurations. From these data c_p values and Stanton numbers are deduced. For constant Mach and Reynolds number the experimental results achieved indicate a strong influence of the total temperature on the Stanton number distribution. For the results presented this behavior is mainly based on entropy layer and viscous interaction effects. A correlation function which takes into account these effects correlates the Stanton numbers achieved for different flow conditions and in different wind tunnels fairly well.

Introduction

THE development of modern re-entry vehicles requires extensive testing in hypersonic test facilities. The results obtained are used for the design process as well as for computational fluid dynamics (CFD) code validation. In the present paper some experimental results are given which were achieved in the Aachen shock tunnel TH2. With a maximum flow velocity of about 3.5 km/s this facility is able to produce flow conditions with vibrational excitation and dissociation of oxygen molecules. During the last few years the Aachen shock tunnel has been intensively used within the Hermes program to study the hypersonic flow around typical re-entry bodies. The measured surface values are transformed into pressure coefficients and Stanton numbers. This allows the correlation of experimental data achieved for different freestream conditions but does not include all of the variables of influence. Particular the Stanton number still shows a strong dependence on Mach and Reynolds number as well as on the shock conditions.

A special correlation function allows these problems to be overcome and the results achieved for different flow conditions and in different wind tunnels to be compared. This is demonstrated for blunt bodies, like a double ellipsoid or a Hermes model, as well as for a relatively thin hypersonic aircraft model.

Hypersonic Model Test

Double Ellipsoid

During the last few years many experiments have been performed in the Aachen shock tunnel where typical re-entry bodies have been measured for pressure and heat flux distributions. From these data pressure and Stanton numbers are deduced by applying a well-developed method¹ to determine the freestream conditions. As a typical example, Fig. 1 shows the Stanton number distribution around the windward side of a double ellipsoid, which has been selected as test case for the Antibes Workshops Part I and II.² It is interesting to compare these results with those achieved for approximately the same Mach and Reynolds number but for different stagnation temperatures. This is presented for the windward side in Fig. 1. For the two lower curves it is obvious that the lower stagnation temperature yields higher Stanton numbers. This difference cannot be explained

by the small deviation of the Mach numbers of the two tests. For the pressure coefficient no such significant deviation has been obtained. Since the difference between the Stanton numbers of the two tests becomes larger with increasing distance from the nose, this may indicate that this is not only due to real gas effects. One has to take into account two other important phenomena, which influence the heat transfer. First, as it is well known, the curved shock around the blunt nose produces an entropy layer which interacts with the boundary layer. This increases the surface heating. Second, for thick boundary layers viscous interaction between the boundary layer and the outer flow takes place. In the downstream direction, compared to the inviscid case, this leads to a stronger pressure decrease which also produces a higher surface heating. There exist some theoretical approaches related to these phenomena. Le Bozec³ proposed a correlation of the Stanton numbers by a relation which was used by Miller et al.⁴ for the heating on biconics. The Stanton numbers are correlated by⁴

$$St_R = St \frac{(\rho_s/\rho_\infty)^{\frac{1}{3}}}{M_\infty \sqrt{C^*/Re_\infty}} = f(x/L) \quad (1)$$

where the Chapman-Rubesin factor

$$C^* = \frac{\mu^* T_\infty}{\mu_\infty T^*} \quad (2)$$

is calculated for a reference temperature T^*

$$T^* = \frac{T_s}{6} \left(1 + 3 \frac{T_w}{T_s} \right) \quad (3)$$

This approach is based on a work performed by Cheng et al.,⁵ who studied the boundary-layer displacement and leading-edge bluntness effects in high-temperature hypersonic flow for flat plates.

From a simplified point of view in Eq. (1) the factor $M_\infty \sqrt{C^*/Re_\infty}$ is caused by the viscous interaction phenomenon, whereas the factor $(\rho_s/\rho_\infty)^{\frac{1}{3}}$ can be attributed to the bluntness effect. The exponent of the density ratio mainly depends on the geometry and on the flow condition to some extent. According to the first-order theory of Cheng et al.⁵ for a flat plate at zero degree incidence and strong bluntness effects the result can be simplified in the following manner:

$$St \frac{(\rho_s/\rho_\infty)^{\frac{1}{3}}}{M_\infty \sqrt{C^*/Re_x}} = f(x/t, \dots) \quad (4)$$

where t is the thickness of the blunt leading edge or nose.

Presented at the AIAA/DGLR 5th International Aerospace Planes and Hypersonics Technologies Conference, Munich, Germany, Nov. 30–Dec. 3, 1993; received Feb. 10, 1994; revision received May 19, 1994; accepted for publication June 15, 1994. Copyright © 1994 by the American Institute of Aeronautics and Astronautics, Inc. All rights reserved.

*Research Scientist, Shock Wave Laboratory.

†Professor, Shock Wave Laboratory. Member AIAA.

‡Test Engineer.

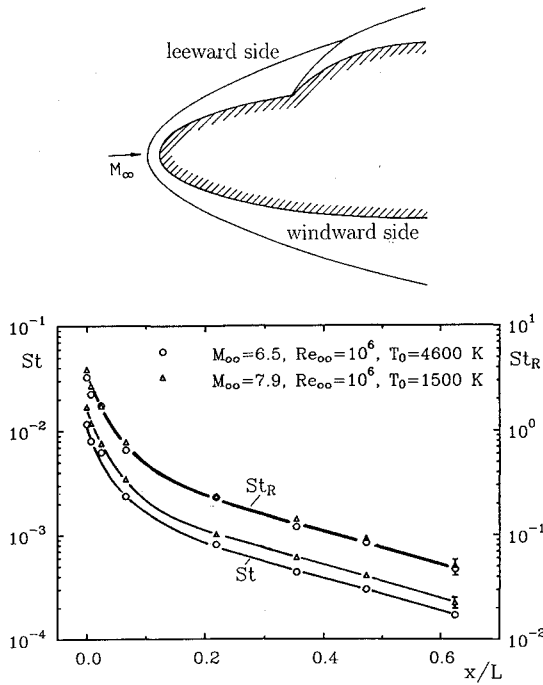


Fig. 1 Original and reduced Stanton numbers for the windward side of the double ellipsoid, $\alpha = 0$ deg.

Based on the Cheng et al.⁵ theory for slender blunt cones Witliff and Wilson⁶ give the following relation:

$$\frac{St(\rho_s/\rho_\infty)^{1/4}}{M_\infty \sqrt{C^*/Re_\infty}} = f(x/L, L/D, \dots) \quad (5)$$

But for this case a comparison with experimental results shows only poor agreement.⁶ From the experimental results for the flow around typical blunt re-entry bodies the authors found

$$St_R^* = \frac{St(\rho_s/\rho_\infty)^{2/3}}{M_\infty \sqrt{C^*/Re_\infty}} = f(x/L, \dots) \quad (6)$$

which results in a slightly improved correlation compared to that of Eq. (1).

Returning to the experiments performed with the double ellipsoid, Fig. 1 also shows the correlated Stanton numbers according to Eq. (1). It is remarkable that the correlated Stanton numbers for both test conditions nearly coincide. The same result is found for correlating the Stanton numbers by Eq. (6). This means that the difference between the two test conditions in the original Stanton numbers is due not only to real gas effects but is mostly due to entropy layer and viscous interaction phenomena. Of course, the ratio wall-to-total temperature also changes with the test condition and in this case it varies from 0.06 to 0.2. To some extent this is also taken into account by the reference temperature T^* and the factor C^* . However, for a cool wall, as is the case for the results presented, the influence of this temperature ratio on the Stanton number is very weak.⁷

Hermes Configuration

Most of the experiments have been performed with real re-entry configurations, like the European Hermes space glider. For this purpose, typically models are used on a scale of 1/55. Special flow conditions are chosen to study the influence of the stagnation temperature or of the viscous interaction. For the windward side some results of these tests are given in Fig. 2. There, a large range of stagnation temperatures, and Mach and Reynolds numbers is covered. For these tests the viscous interaction parameter

$$\chi = \frac{M_\infty^3}{\sqrt{Re}} \sqrt{C^*} \quad (7)$$

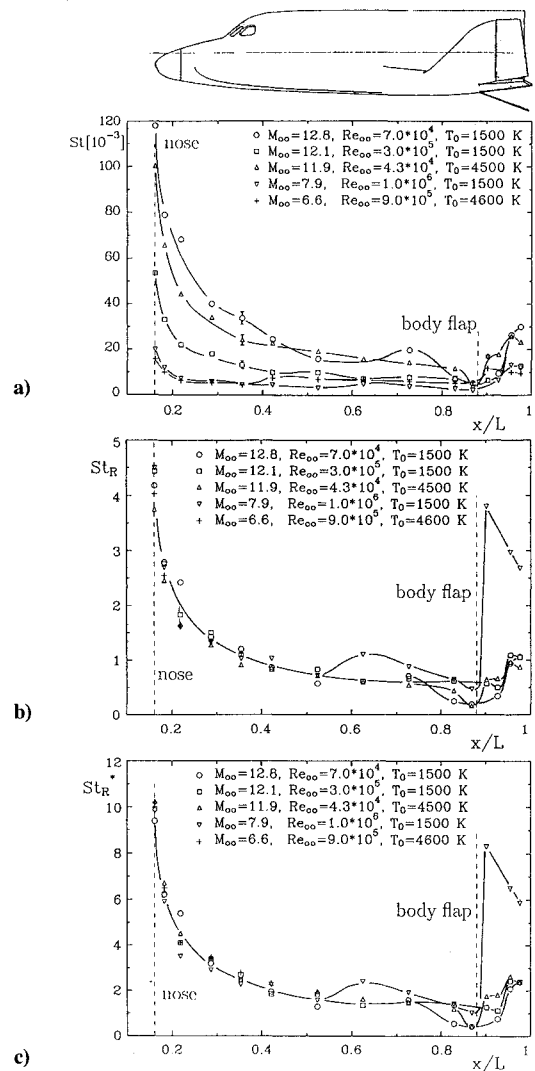


Fig. 2 Stanton number distributions for the windward side of Hermes, $\alpha = 40$ deg, $\delta_F = 20$ deg: a) original Stanton number, b) correlated Stanton number according to Eq. (1), and c) correlated Stanton number according to Eq. (6).

varied from 0.3 to 7.5, which means from very weak to very strong viscous interaction. Figure 2a shows the dependence of the original Stanton number on the various test conditions. At the nose the strongest influence of the flow conditions is observed, where the Stanton number typically changes by a factor of 5–10. From these data according to Eq. (1) the correlated Stanton numbers St_R have been computed and are plotted in Fig. 2b. They show a fairly good correlation. Of course, the remaining scatter is also caused by uncertainties in the determination of the freestream conditions for the various flow conditions. The correlated Stanton numbers according to Eq. (6) are presented in Fig. 2c. As mentioned earlier, this relation yields a slightly improved correlation, especially at the nose. The third gauge at $x/L = 22\%$ shows a bigger scatter than the other ones. At the end of the test campaign it turned out that this gauge had not always worked properly. The presentation of the Stanton number in correlated form helps to detect the significant differences in flow behavior of the various experiments. On the body flap, e.g., for $M_\infty = 7.9$, the correlated Stanton number shows a remarkably higher level than for the other tests. But for this test at $x/L = 60\%$, a weak transition of the boundary layer occurred. This is not very clear from the original Stanton number distribution, Fig. 2a. For this test the transitional boundary layer leads to much higher heat fluxes on the flap. Compared to the other tests, this is not clearly represented in the original Stanton number plot, but for the correlated one it is. Shortly in front of the body flap the scatter of the correlated Stanton numbers slightly increases. This is due to the formation of a

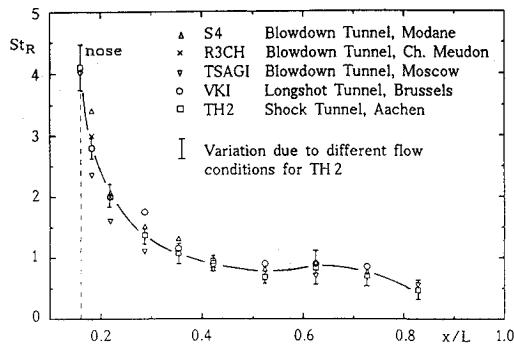


Fig. 3 Comparison of correlated Stanton number distribution achieved in different wind tunnels, Hermes model, $\alpha = 40$ deg, windward side.

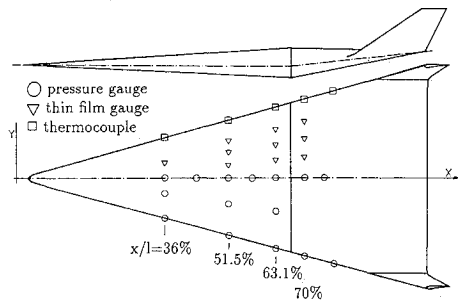


Fig. 4 ELAC geometry and location of gauges.

separation bubble in front of the flap. Of course, this phenomenon is not taken into account in the presented correlation relations, which are strictly valid for attached laminar boundary-layer flow.

This Hermes model was also measured in several test facilities of different kinds and sizes. Correspondingly, the flow conditions of these tests varied nearly in the same range as that indicated in Fig. 2. Furthermore, models of different size have been used. Nevertheless, the comparison of the correlated Stanton number distributions in Fig. 3 shows a fairly good agreement. For the tests performed in the Aachen shock tunnel, from Fig. 2b for each position, an average correlated Stanton number and a typical margin resulting from the different flow conditions could be given. Of course, the comparison of these results is influenced by some uncertainties, which may be responsible for the remaining scattering. These uncertainties are due to different methods used in the test facilities to determine the freestream properties, to perform the heat flux measurements, and to calibrate the heat flux gauges, etc. Furthermore, there may be small geometrical deviations of the different models. Taking into account all these error sources the agreement achieved is good.

Hypersonic ELAC Configuration

ELAC is a reference configuration of a special research center (Sonderforschungsbereich 253) "Fundamentals of Design of Aerospace Planes" at the Aachen University of Technology. A delta wing was chosen to represent the lower stage of a two-stage space transportation system. It has elliptical cross sections, where the geometry is defined as simply as possible to allow for a simple numerical treatment of the flow. Details of this project and experimental and numerical results are given in Ref. 8. The general shape of ELAC is shown in Fig. 4.

In the context of this paper the authors will concentrate on the heat transfer measurements, which have also been performed along the wing leading edge. Compared to re-entry bodies, ELAC represents a relatively thin body where the bluntness of the nose is much smaller than the other dimensions and the shock strength along the leading edge in streamwise direction does not change very much. Thus, for the surface heat transfer along the leading edge no entropy layer effects should occur, since they are typical for the double ellipsoid or Hermes. Therefore, the density ratio across the shock should not have any influence on the correlation of the Stanton number, which

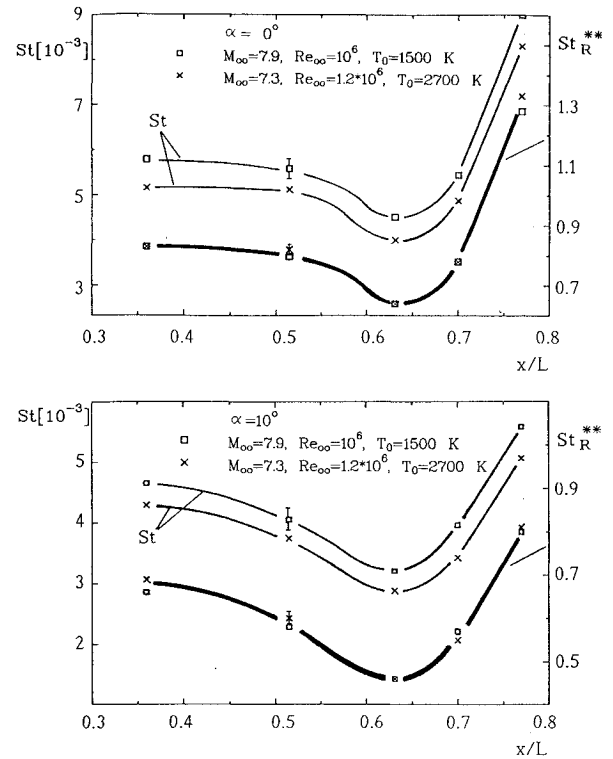


Fig. 5 Stanton number distribution along the wing leading edge for $\alpha = 0$ and 10 deg.

for this case results in the following correlation:

$$St_R^{**} = St \frac{\sqrt{Re_{\infty}/C^*}}{M_{\infty}} = f(x/L) \quad (8)$$

For two angles of attack and two test conditions, the original and correlated Stanton numbers are presented in Fig. 5. Since the heat transfer along the wing leading edge is proportional to $1/\sqrt{r}$, where r is the nose radius of the leading edge, first the Stanton number decreases to reach a minimum at the junction between the front and afterbody. Behind the junction, the nose radius decreases and so the heat flux and, therefore the Stanton number increases.

The two upper curves in Fig. 5 clearly show the difference in the Stanton number distributions for the two test conditions. This is mainly caused by the different stagnation temperatures. Since for this model geometry no strong entropy layer effects are expected, the Stanton number should correlate according to Eq. (8). This correlated Stanton number is also presented in Fig. 5, and it shows a good correlation for the two test conditions and the two angles of attack. Unfortunately, until now no further experiments for other flow conditions have been performed with this configuration. But we think that this example and the former ones clearly demonstrate the influence of the viscous interaction and the nose bluntness on the heat transfer, as well as the usefulness of the correlation functions presented.

Conclusions

A shock tunnel has been used to study the hypersonic flow around typical re-entry bodies and space planes. From surface pressure and heat transfer measurements, pressure coefficients and Stanton numbers are deduced. The experimental data, achieved with different model geometries and for various flow conditions, could be correlated quite well by relations which have been found for blunt cone flows. The correlation takes into account entropy layer effects caused by curved shocks and viscous interaction phenomena. Variation of the stagnation temperature for constant Mach and Reynolds number has a strong influence on these two effects. For a thin body, where the entropy layer effect is not very strong, its influence could be separated from the correlation relation. The corresponding experimental data also show a good correlation.

Acknowledgments

The upgrading of the shock tunnel and most of the experiments have been funded by CNES and Dassault Aviation. The experiments with the ELAC configuration were performed as part of the Aachen special research center (Sonderforschungsbereich 253) "Fundamentals of Design of Aerospace Planes," which was established by the German Science Foundation. The authors are grateful to M. Vetter who performed the experimental work.

References

- ¹Olivier, H., "An Improved Method to Determine Free Stream Conditions in Hypersonic Facilities," *Shock Waves*, Vol. 3, No. 2, 1993, pp. 129-139.
- ²Vetter, M., Olivier, H., and Grönig, H., "Flow over Double Ellipsoid and Sphere—Experimental Results," *Hypersonic Flows for Re-entry Problems*, Proceedings of the INRIA-GAMNI/SMIAI Workshop on Hypersonic Flows for Re-entry Problems, Pt. II, edited by R. Abgrall et al., Antibes, France, 1991, pp. 489-500.

³Le Bozec, A., private communication, Dassault Aviation, Dept. for Experimental Aerodynamic, Vélizy, France, 1993.

⁴Miller, C. G., Gnoffo, P. A., and Micol, J. R., "Heat-transfer Distributions for Biconics at Incidence in Hypersonic Hypervelocity Real-gas Flows," *Proceedings of the 14th International Symposium on Shock Tubes and Waves*, edited by R. D. Archer and B. E. Milton, New South Wales Univ. Press, Sydney, Australia, 1983, pp. 333-341.

⁵Cheng, H. K., Gordon Hall, J., Gobian, T. C., and Hertzberg, A., "Boundary-layer Displacement and Leading-edge Bluntness Effects in High-temperature Hypersonic Flow," *Journal of Aerospace Sciences*, Vol. 28, No. 5, 1961, pp. 353-381.

⁶Witliff, C. E., and Wilson, M. R., "Heat Transfer to Slender Cones in Hypersonic Air Flow, Including Effects of Yaw and Nose Bluntness," *Journal of Aerospace Sciences*, Vol. 29, No. 7, 1962, pp. 761-774.

⁷Van Driest, E. R., "Investigation of Laminar Boundary Layer in Compressible Fluids Using the Crocco Method," NACA TN 2579, Jan. 1952.

⁸ZFW, "Fundamentals of Design of Aerospace Planes," *Journal of Flight Sciences and Space Research*, Vol. 17, No. 2, 1993, pp. 71-156.

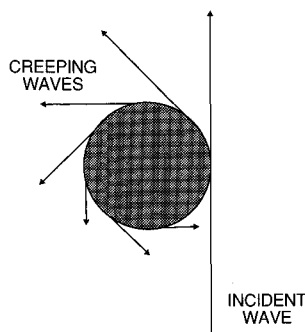
Tactical Missile Aerodynamics: General Topics

Michael J. Hemsch, editor

This volume contains updated versions of three chapters from the first edition and six new chapters covering such topics as a history of missiles, system design, radar observables, unsteady flows, and store carriage and separation. More than 500 figures and five color plates support the text.

Contents include: Historical Review of Tactical Missile Airframe Developments; Aerodynamic Considerations for Autopilot Design; Radar Observables; Visualization of High-Angle-of-Attack Flow Phenomena; Low Aspect Ratio Wings at High Angles of Attack Inlets; Waveriders, and more.

1992, 700 pp, illus, Hardback
ISBN 1-56347-015-2
AIAA Members \$64.95
Nonmembers \$79.95
Order #: V-141(945)



Tactical Missile Aerodynamics: Prediction Methodology

Michael R. Mendenhall, editor

This book contains updated versions of nine chapters from the first edition and new chapters on drag prediction, component build-up methods, Euler methods, and Navier-Stokes solvers. Special attention is paid to nonlinear flow phenomena and unconventional airframe shapes. Eight color plates and more than 540 figures are included.

Contents include: Tactical Missile Drag; Drag Prediction Methods for Axisymmetric Missile Bodies; Introduction to the Aerodynamic Heating Analysis of Supersonic Missiles; Component Build-Up Method for Engineering Analysis of Missiles at Low-to-High Angles of Attack, and more.

1992, 700 pp, illus, Hardback
ISBN 1-56347-016-0
AIAA Members \$64.95
Nonmembers \$79.95
Order #: V-142(945)

Save when you buy the complete set:
AIAA Members \$120
Nonmembers \$145
Order #: V-141/142(945)

Place your order today! Call 1-800/682-AIAA



American Institute of Aeronautics and Astronautics

Publications Customer Service, 9 Jay Gould Ct., P.O. Box 753, Waldorf, MD 20604
FAX 301/843-0159 Phone 1-800/682-2422 9 a.m. - 5 p.m. Eastern

Sales Tax: CA residents, 8.25%; DC, 6%. For shipping and handling add \$4.75 for 1-4 books (call for rates for higher quantities). Orders under \$100.00 must be prepaid. Foreign orders must be prepaid and include a \$20.00 postal surcharge. Please allow 4 weeks for delivery. Prices are subject to change without notice. Returns will be accepted within 30 days. Non-U.S. residents are responsible for payment of any taxes required by their government.